2020

The Characterization of Inflammatory Extracellular Vesicles

Barak Balva

LOYOLA UNIVERSITY CHICAGO

THE CHARACTERIZATION OF INFLAMMATORY EXTRACELLULAR VESICLES

A THESIS SUBMITTED TO

THE FACULTY OF THE GRADUATE SCHOOL

IN CANDIDACY FOR THE DEGREE OF

MASTER OF SCIENCE

PROGRAM IN INFECTIOUS DISEASE AND IMMUNOLOGY

BY

BARAK BALVA

CHICAGO, IL

AUGUST 2020

ACKNOWLEDGEMENTS

I would like to thank all of the people who made this submission possible. First and foremost, my mentor Dr. Edward Campbell, who provided an educational, encouraging and exciting environment to be a part of on a daily basis. Additionally, my committee members: Dr. Francis Alonzo, Dr. Thomas Gallagher, and Dr. Gopal Gupta, whose inputs have improved the quality of this project and my abilities as a scientist. I would like to thank all my lab members, but specifically Dr. Sarah Talley, who taught me much about what I know regarding inflammation and inflammasomes, and Virginia Zwikelmaier, who trained me throughout my early months with the lab.

I would also like to thank my friends for understanding when I couldn't grab a beer on Saturday afternoons because I had timepoints to attend to. And finally, my family, who without their support in pursuing my education further I wouldn't be currently typing this section.

TABLE OF CONTENTS

LIST OF FIGURES

LIST OF ABBREVIATIONS

Aβ	Amyloid Beta
AD	Alzheimer's Disease
ALIX	ALG-2 Interacting Protein X
ASC	Associated Speck-like protein with a CARD
ATP	Adenosine Tri-Phosphate
BFA	Brefeldin-A
DAMP	Damage Associated Molecular Pattern
EBV	Epstein Barr Virus
ER	Endoplasmic Reticulum
EV	Extracellular Vesicle
KO	Knock-Out
LEL	Large Extracellular Loop
LRR	Leucine Rich Regions
MV	Microvesicle
MVB	Multivesicular Body
NLR	Nod-Like Receptor
NOD	Nucleotide-binding and Oligomerization domain
PAMP	Pattern Associated Molecular Pattern
PD	Parkinson's Disease
PM	Plasma Membrane
PrP	Prion Protein
PRR	Pattern Recognition Receptor

PS	Phophatidylserine
PYD	Pyrin Domain
RA	Rheumatoid Arthritis
ROS	Reactive Oxygen Species
TGN	Trans-Golgi Network
TLR	Toll-Like Receptor
TSG101	Tumor Susceptibility Gene 101
UC	Ultracentrifugation

CHAPTER ONE

INTRODUCTION

Protection of Self from a wide range of pathogens is controlled by immunity, divided into two subgroups: innate and adaptive [1]. One of the driving factors behind innate immunity is the early response of inflammation, which is induced by either microbial infection or tissue damage. An inflammatory response is often beneficial in controlling infections and protecting an individual from foreign invaders. When uncontrolled, a hyperinflammatory response can lead to a plethora of disorders, including Parkinson's Disease (PD), Alzheimer's Disease (AD), and Rheumatoid Arthritis (RA) among many others [2]. Understanding the factors that cause this uncontrolled inflammation has been a popular topic within research, as further understanding can lead to pathogenic control and potential drug targets.

Another topic within the field of biology that has gained considerable prominence in the last few decades is autophagy, described as an intracellular degradative process responsible for the degrading or recycling of cellular materials [3]. The lysosome is the key organelle responsible for this degradative process, and impairments of the lysosome can lead to numerous disorders [4]. Within the many avenues of autophagy, the ones involving extracellular vesicle (EV) secretion have been of high interest due to cells being able to exchange materials from one to the other via EVs [5]. EVs have been found in association with multiple neurodegenerative disorders, including the previously mentioned PD and AD [6].

The association between EV secretion and inflammation has been appreciated within the last decade, and it is this relationship that has intrigued us as a lab. Caspase-1, an effector

protease of the inflammasome complex that is formed upon a diverse range of signals, has been shown to drive the secretion of a wide volume of proteins. Unlike the conventional ER- Golgi secretory pathway, caspase-1 drives protein secretion via non-conventional methods, including EVs [5]. Hence, we have two very different biochemical processes—inflammation and protein secretion via EVs—that have relevant roles within disease pathogenesis and amongst themselves. Additionally, it is the cargo associated with EV-secretion that interests us a lab. Different cargo can either exert biological functions on neighboring cells, or in association with EVs can potentially represent biomarkers for various diseases.

The goals of this research consist of further elucidating the mechanisms behind these two distinct biochemical pathways, and how the association between the two has further implications to disease pathogenesis and progression. Using an imaging-based method that allows for analyzation of EV populations on an individual EV level, we can further characterize EV groups under different stimuli, look at different cargos associated with EVs, and label EVs via staining for different markers—some well-established and some more recently appreciated. Through this efficient and relatively fast approach, we can further elucidate the role EVs have within inflammation and provide exciting new approaches for studying two very integral topics within the field of Biology.

CHAPTER TWO

REVIEW OF THE LITERATURE

Inflammation

Inflammation, a general innate immune system response, is a crucial aspect of our early host defense against numerous pathogens. A balance of inflammatory responses is essential to maintain, as uncontrolled inflammatory responses drive the progression of many diseases. The innate immune system is the first line of defense against foreign invaders. Pattern-Recognition Receptors (PRRs) embedded on the surface of many cell types recognize specific microbial cell patterns, categorized as Pattern Associated Molecular Patterns (PAMPs) and Damage Associated Molecular Patterns (DAMPs) [7]. The recognition of PAMPs and DAMPs by PRRs leads to downstream inflammatory effects, most notably the formation of inflammasomes, and thus partake in the process of eliminating foreign pathogen invaders.

Inflammasomes.

The inflammasome was first described in 2002, when a group discovered a multiprotein complex consisting of NLRP1, ASC, and pro-inflammatory caspases that came together upon inflammatory induction [8]. At the time, it was known that caspase-1 cleaved pro-IL-1β to its mature form, however the mechanism behind that wasn't fully understood. Inflammasomes are thus defined as multi-protein complexes made up of intracellular apoptosis-associated speck-like protein containing a CARD (ASC) and a sensor NLR. Deemed as the sensors of innate immunity, their formation and activation are processed as a response to infectious 'attacks',

presenting themselves to cell surface receptors as the aforementioned PAMPs and DAMPs (12). Activation of caspase-1, a cysteine protease involved in cleaving pro-inflammatory cytokines such as IL-1β and IL-18 to their mature forms, is promoted by NLR family members such as NLRP1, NLRP3, and NLRC4 [9,10]. The assembly and activation of each respective inflammasome is dependent on various environments and stimuli. The most well studied of all inflammasomes, and the one that will be the focus of this research, is NLRP3.

Interleukin-1β (IL-1β).

Interleukin-1β is a potent pro-inflammatory cytokine, and the main cytokine that will be focused on throughout this research. It has a beneficial role mediating a host's response to many infectious agents [8,9,11]. IL-1β is produced and processed by cell lines of the monocytic lineage, including but not limited to monocytes, macrophages, and dendritic cells. It is a 31 kDa sized protein in its inactive pro-form, and is broken down into a 17 kDa sized protein in its mature active form. Upon LPS stimulation, IL-1β mRNA levels are greatly amplified after only 15 minutes, and the pro-form of IL-1β accumulates in the cell until inflammasome activation takes place [12]. Many processes can be involved for IL-1β release from the cell, including exocytosis of secretory lysosomes, shedding of plasma membrane microvesicles, etc.. Like many cytokines, it does not contain a signal peptide, and is thus secreted from cells via the non-conventional secretory pathway which will be discussed later on. This was first suggested by a group that treated cells with brefeldin A (BFA). BFA causes the collapse of the TGN, which is integral for conventional protein secretion. Upon inflammatory stimulation, IL-1β was still released from cells, thus suggesting an alternative route for release [13]. Upon release, this cytokine has a role in various cellular processes, including cellular differentiation, proliferation, and pyroptosis. IL-1β

released from inflammatory-induced cells is one the indicators we will use to confirm NLRP3 inflammasome activation.

NLRP3 Inflammasome.

NLRP3 requires two steps for its activation and downstream effects: a priming first signal and a secondary signal. The priming signal, or signal 1, is provided via microbial agents, such as lipopolysaccharide (LPS), or endogenous cytokines, like IL-1β, which drive the activation of transcription factor NF-KB [7]. The activation of NF-KB leads to the upregulation of NLRP3, as well as pro-inflammatory cytokines such as IL-1β and IL-18. The activation signal, or signal 2, is caused by a plethora of agents, including ATP, monosodium urate, β-glucans, nigericin, and other components like RNA viruses [5]. ATP is often the agent we use to induce this activation signal. A well-established DAMP, exogenous ATP is often hydrolyzed by endonucleases [14]. However, upon significant cellular damage and extracellular release, the levels of extracellular ATP are far greater than what can be hydrolyzed. Thus, ATP can be recognized by macrophages as a danger signal, and aids in inflammasome activation. P2X7 is a channel present on many cell types, including macrophages, and ATP interacts with P2X7 by binding to it, leading to channel dilation. This dilation also drives increased ROS within the cell, which also further drives NLRP3 inflammasome activation [7]. The NLRP3 protein itself is composed of three parts: an amino terminal pyrin domain (PYD), a central nucleotide-binding and oligomerization domain (NOD), and C-terminal leucine rich domain (LRR). It is the pyrin domain of NLRP3 that interacts with the pyrin domain of ASC upon inflammasome activation [15]. Once associated with NLRP3, ASC recruits caspase-1 to the complex, thus forming the NLRP3 inflammasome. Upon proximity, caspase-1 auto-cleaves itself to its active form, and then proceeds to cleave pro-

inflammatory cytokines. This leads to the downstream effects of NLRP3 inflammasome activation. A simplified version of this process is illustrated in Figure 1 below.

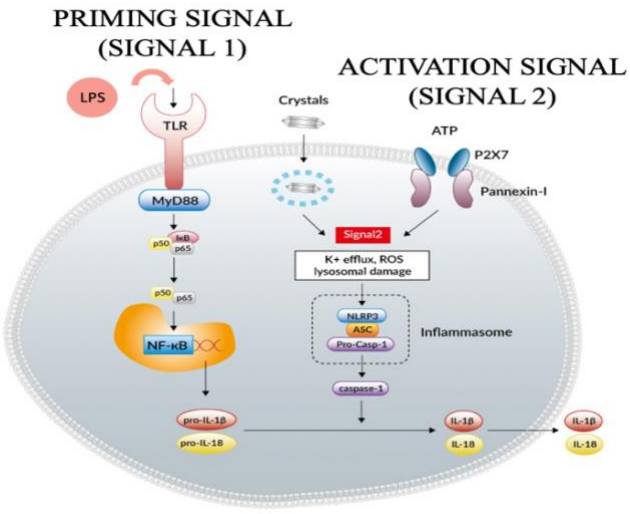

Figure 1. Simplified NLRP3 Inflammasome Activation (7). A priming signal, such as LPS, interacts with surface PRR, such as TLR7, which leads to activation of NF-KB and the upregulation of pro-inflammatory cytokines such as pro-IL-1β and pro-IL-18. These pro-inflammatory cytokines accumulate in the cytoplasm, reaching a max upregulation about 4 hours after LPS stimulation. A secondary signal, either in the form of ATP, monosodium urate, nigericin, etc.. causes the NLRP3 inflammasome to form, leading to pro-caspase-1 autocleavage to it's mature caspase-1 form, which then proceeds to cleave pro-inflammatory cytokines into their mature forms, for eventual release from the cell and subsequent inflammatory cascade.

The NLRP3 inflammasome has been implicated in numerous disorders. In Alzheimer's, Aβ aggregates have been shown to activate NLRP3-ASC inflammasome, which further amplifies amyloid pathology *in vivo* [16]. Specifically, Aβ acts as the secondary activation signal, similar to ATP. Additionally, Tau has also been shown to activate the NLRP3 inflammasome in a prion-like fashion, and ASC deficiency in mice caused an inhibition of this exogenously seeded Tau pathology. Epstein-Barr virus (EBV), while usually presenting itself asymptomatically in most patients, is an oncogenic virus responsible for many cancers upon reactivation later in life, and its reactivation from its latent state has been attributed to excessive NLRP3 inflammasome activation [17]. In the same study that described how Aβ can activate the

NLRP3 inflammasome, they also noted that ASC specks are released from inflamed microglial cells, with the potential to propagate inflammation.

Apoptosis-Associated Speck-Like Protein Containing a CARD (ASC).

ASC is a 22 kDa protein which was first identified as having a caspase-recruiting domain. This protein acts as the bridge between NLRP3 and caspase-1. ASC polymers themselves are what bring pro-caspase-1's into close proximity with each other in the inflammasome complex, which thus mediates the previously mentioned auto-cleavage to active caspase-1 [18]. Characteristic speck formation of ASC are strong indicators of inflammasome activation. Independent of the effects of ASC in the context of an inflammasome, ASC is also released outside phagocytic cells into the cytosol. In the cytosol, ASC can still be visualized as specks, and these specks have been reported to have prion-like properties and can promote inflammation themselves (12) [18]. To understand the potential effects of ASC as a prion-like protein, a better understanding of prions needs to take place.

Prion Proteins.

Prions are cell surface proteins expressed on numerous cell types in various organs, specifically those relating to the peripheral and central nervous systems [19,20]. Their presence on cell surfaces increases as brain development progresses in humans. However, there is some debate regarding the presence of prion proteins in older individuals. In post-mortem individuals, there is a decrease in prion proteins in older individuals, while in mice there is an increase [21]. Regardless, the exact function of prion proteins is not fully understood. KO PrP_C in mice prevented progression of scrapie transmission, a prion disease, which is unsurprising as the process is dependent on prion proteins. However, no other phenotypes were observed, which is surprising in itself as the sequence and structure of prion proteins are well conserved in many

animal species. It has been suggested that PrP^{c} is associated with ER stress, as PrP^{c} is overexpressed upon addition of agents that induce ER stress. ER stress is caused by an accumulation of unfolded or misfolded proteins, which increases expression of chaperone proteins that aid in folding, and inhibits protein synthesis to give cells time to correct misfolded or unfolded proteins. The main area of focus regarding prion proteins is their role in disease, specifically neurodegenerative disorders. PrP is able to conformationally change from its cellular state, PrP^{c}, to its insoluble isoform PrP^{Sc}, which is resistant to proteinase K degredation[22]. Misfolded prions can then transfer from cell to cell, thus inducing conformational changes on other normally folded prion proteins, thus aiding in disease propagation. As our lab studies neurodegenerative disorders, it is important to further understand inflammasome proteins, like ASC, which have the potential to act in a prion-like manner. Additionally, we also study processes of protein secretion from cells. Cells that undergo inflammasome activation are responsible for an increase in protein secretion, and EV release as well. To further understand the potential role ASC has as it is released from cells, we need to first delve into the different avenues of protein secretion.

Autophagy and Protein Secretion

Autophagy is a self-degradative process that is important for recycling cellular material, responding to nutrient requirements and stressors, removing damaged organelles, and removing aggregated or misfolded proteins [23,24]. Overall, the process begins with an autophagosome (likely derived from the lipid bilayer of the ER) consuming cellular cargo, be it organelles, proteins, protein aggregates, etc.. Upon engulfment, the autophagophore becomes a double membraned autophagosome. This autophagosome later fuses with the lysosome, which degrades the consumed cargo. Proteases within the lysosome break down the products upon fusion, where

they can later on be reused or discarded from the cell. An illustration of the main types of autophagy are shown in Figure 2 below. The autophagy-lysosome system is vital for controlling infection and eventual immunity, in terms of breakdown of foreign microbial agents and antigenic presentation to immune cells. Beyond a relationship between autophagy and immunology that can be appreciated, autophagy is also crucial for protein secretion from the cell. Additionally, it has been suggested that EVs are cleared from cells via the autophagy-lysosome pathway, and thus a clear understanding of degradation and protein secretion are of high importance to better understand EVs [25].

Classical/Conventional Secretory Pathways.

Conventionally secreted proteins are categorized and labeled by a signal peptide on the N-terminal end, which directs the proteins from the ER to the Golgi apparatus [14]. From there, proteins are moved to the trans-Golgi network (TGN), and eventually to the plasma membrane [11]. Regulatory proteins are responsible for control throughout this process. Up until the last two decades, this classical protein secretion pathway has been thought of as the standard for protein secretion.

Non-Classical/Non-Conventional Secretory Pathways.

Proteins secreted from cells using pathways that don't involve ER-to-Golgi transport are categorized in the non-classical/non-conventional secretory pathway. There are two main subgroups of non-conventional protein secretion: those that do not contain the aforementioned signal peptide on the N-terminal end, and those that do have a signal peptide but bypass the Golgi [11]. Most of the proteins that are secreted via this pathway aren't done so under normal cellular conditions. Rather, their secretion is often induced by cellular stress, mechanical stress, and inflammation. Activation of P2X7 channels, which as mentioned previously interact with

extracellular ATP and drive NLRP3 inflammasome activation, are largely responsible for changing cellular morphology. It is under these morphological changes that there is an increase of proteins trafficked to the membrane to be released via vesicles [14]. Many cytokines are released in this pathway, as they do not contain signal peptides [11].

Extracellular Vesicles

As an overall generalized term, EVs refer to membrane bound vesicles containing various molecules[26], further categorized by their size, origin, release pathways, and environments [25]. Once thought to be cell debris that have no additional value or function upon release [27], EVs are now appreciated as having an important role in many biological processes, including transfer of proteins and RNA from cell to cell, thus suggesting a role in intercellular communication [26]. EVs can be broken down into the following groups: apoptotic bodies, microvesicles, and exosomes, as illustrated in Figure 2 below [28,29].

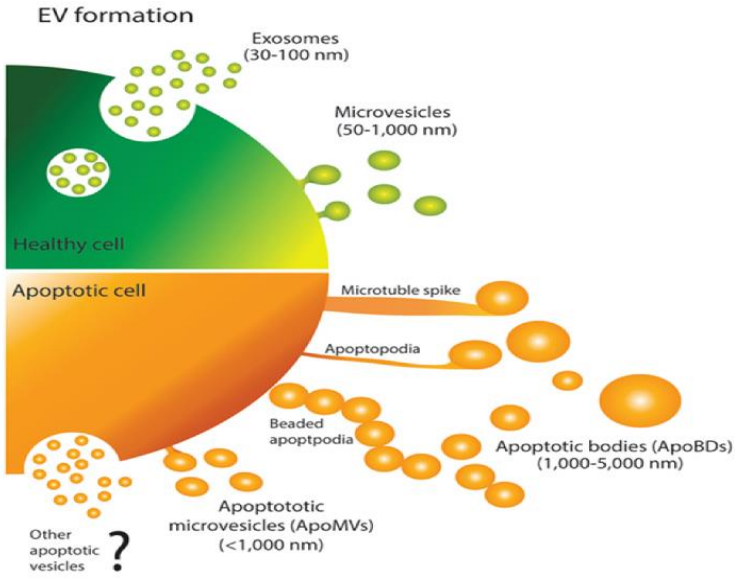

Figure 2. Breakdown of EV Formation (28). The three main categories of EVs are illustrated, showing the origin of their formation. Apoptotic bodies are released from dying cells. MVs are released from budding of the plasma membrane. Lastly, exosomes are released from endocytic vesicles fusing with the plasma membrane, releasing their contents.

Apoptotic Bodies.

Apoptotic bodies were the first categorized group of EVs, and have been described as EVs released from cells undergoing apoptosis [28]. An appreciation for EVs released from healthy cells has been well established in the field, however apoptotic bodies have been mostly overlooked throughout the growing understanding of EVs in the field. Apoptotic bodies are usually within the range of 1-5 µm, although some have also been mentioned to be smaller than 1 µm. Upon apoptosis, dead cells are either cleared by phagocytes as whole cells, or as fragments—which include apoptotic bodies [30]. Some phagocytes can't consume the full dead cell due to sheer size, which places an even bigger importance on cells abilities to release apoptotic bodies during apoptosis. Apoptotic bodies have also been shown to have a role in recruiting phagocytes to the site of apoptosis for clearance using 'find me' signals, including release of factors such as ATP, which as mentioned before can be recognized by macrophages as a danger signal and elicit NLRP3 activation. This clearance under normal, healthy physiological conditions is paramount to maintaining homeostasis, and individuals that aren't able to clear apoptotic cells have been linked to inflammatory diseases and autoimmunity. Apoptotic bodies can also assist in antigen presentation via MHC class II, and thus have the ability to stimulate CD4+ T cells [31].

Microvesicles.

Microvesicles, the next subgroup of EVs, are usually between 100 nm and 1 µm in size. They express phosphatidylserine (PS) on their surface, as confirmed via annexin staining, although there have also been PS negative MVs [3233]. They characteristically are formed by outward budding of a cell's plasma membrane, so their content is primarily composed of cytosolic and membrane associated proteins. They also have been suggested to require actin and

microtubules for their release, and such components can also be associated with their release. Uptake of MVs by recipient cells has been acknowledged as an energy dependent process, as a decrease in uptake has been observed under conditions with lower temperatures.

Exosomes.

Exosomes are the last subgroup of EVs, and while there has been some debate regarding the similarities between exosomes and MVs, they are a separate class of themselves and do have distinct differences. The defining difference between exosomes and MVs is that while MVs bud outwards from the cytosol to the PM, exosomes are secreted from multivesicular bodies, or MVBs, which are late endosomes[26,29,32–34]. As mentioned previously discussing autophagy, endosomal structures are formed containing cargo that can later fuse with the lysosome, and thus get degraded. In this case, there is no fusion with the lysosome: instead, late endosome fuses with the PM and releases its content to the extracellular space. While the exact details of what deems MVBs for extracellular release vs fusion with the lysosome for degradation is still up for debate, it has been shown that in nutrient starved cells, MVBs are re-routed for degradation as opposed to extracellular release, so the cellular environment plays a role in exocytosis. Exosomes are usually smaller than MVs, and are between 40-150 nm in size.

Tetraspanins.

Due to the origin and distribution of various classes of EVs, it doesn't come as a surprise that different classes have their own distinct markers. However, there are pan-EV markers that span all EVs. Tetraspanins are a protein superfamily that act as transmembrane proteins, with large extracellular loop (LEL) that acts as its most antigenic feature [35]. Of the tetraspanins, the three most commonly used to identify EVs are CD9, CD63, and CD81. A group in 2016 subjected EVs released from human primary monocyte derived dendritic cells to various

ultracentrifugation (UC) techniques: 2000g, 10000g, and 100,000g [36]. The 100k UC technique is accepted to yield a pellet of mostly exosomes, ranging in size from 50-150nm, which is what they saw. The 2k technique yielded mostly larger sized EVs (>200nm), while 10k technique yielded EVs closer in distribution to the 100k. When they performed a Western Blot of proteins from the different centrifugations, they noted that the 100k pellet had strong bands for all three tetraspanins, however CD9 and CD63 were also present in the 2k and 10k pellets as well. There was some hope that tetraspanins could become a specific exosome EV marker, however due to these proteins being expressed on the cell membrane, they can also very easily be incorporated into other subgroups of EVs that originate from cell budding [37]. A breakdown of tetraspanin distribution along the cell membrane is shown in the figure below.

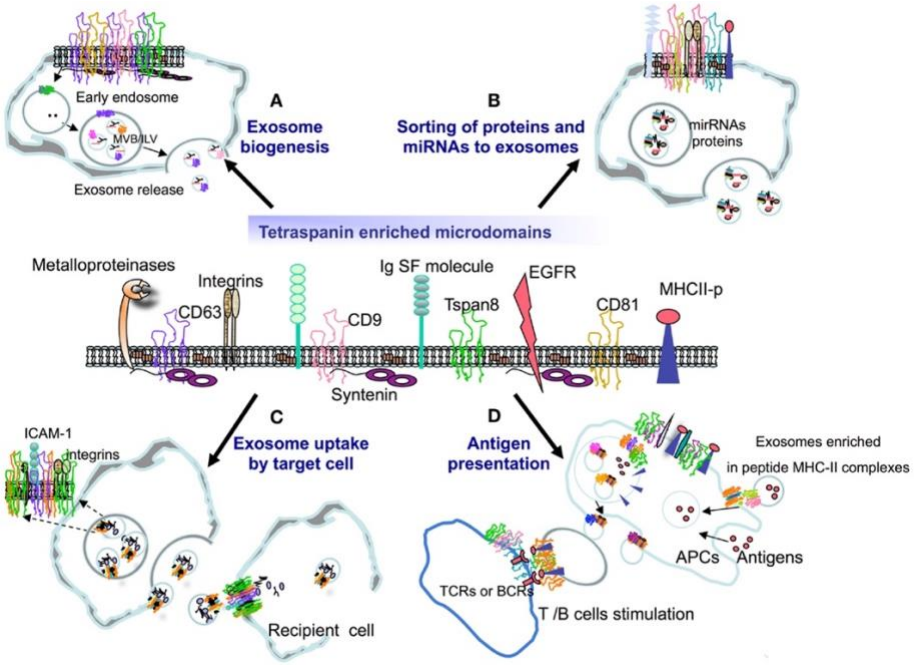

Figure 3. Representation of Tetraspanin Distribution along PM (38). Localization and how tetraspanins span the plasma membrane are clearly illustrated, as well as other membrane markers that can be incorporated into EVs prior to release from cell. Additionally, the importance of these markers for fusion with target cells is also shown under section C.

Other EV Makers.

Digressing from pan-markers, there are certain proteins that are associated with certain EV subgroups based on their origin and biogenesis. Exosomes, for example, have proteins associated with endosomal sorting complex required for transport, or ESCRT, which include ALG-2 interacting protein X (ALIX) and tumor susceptibility gene 101 (TSG101)[39]. ESCRT proteins help with sorting ubiquitinated proteins to their designated MVBs, and also assist with exocytosis [40]. A proteomic analysis of different markers for different EVs sorted by sizes and various centrifugation techniques is visualized in the figure below.

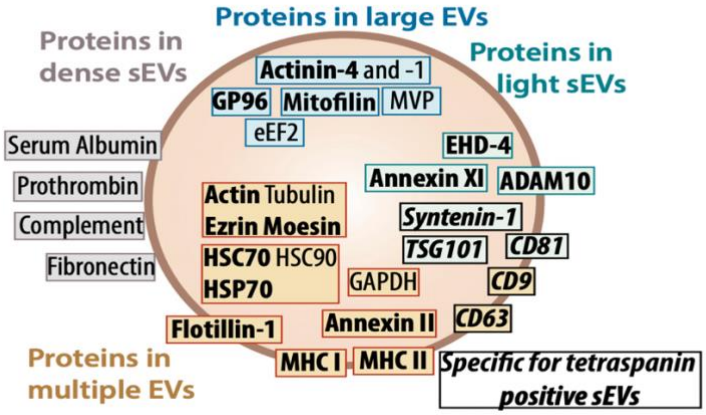

Figure 4. EV Subgroup-Specific Markers (41). As illustrated, tetraspanins (including CD9, CD63, and CD81) are present in multiple EV subgroups, however CD81 is somewhat more concentrated in smaller EVs. Additional markers present on multiple EVs are MHC-I/II, Heat Shock Proteins, Annexin, etc..

Glycobiology and Lectins.

Like EV studies themselves, carbohydrate function in the context of cellular communication was not fully appreciated until the last few decades. Bound to lipids and proteins as glycans, carbohydrate subgroups are now accepted to have important roles as information carriers within cellular trafficking [42]. It is also appreciated that glycoconjugates are involved in EV biogenesis and play a role in their recognition by target cells and their uptake. Additionally,

there are alterations to glycome composition of cells in various disease states, which is another reason why a precise way to label and analyze EVs based on their glycan composition can be hugely beneficial as disease biomarkers. Nearly half of all proteins are glycosylated, and individual proteins can have many different glycosylation sites. The question then becomes: how do we best analyze and label these carbohydrate structures? The answer to this rests within Lectins, which are carbohydrate binding proteins. Lectins recognize and bind to different glycan epitopes on various structures. There are numerous types of lectins, and different lectins will bind to certain cell types under certain conditions depending on their glycan composition. EVs themselves have a defined glycan distribution, and thus utilizing lectins as an EV marker tool has been of great excitement within the field and our lab.

Galectins are a subgroup of lectins which specifically bind β-galactosyl containing glycoconjugates, and they are the most highly expressed subgroup of lectins in all organisms [43]. Studies have shown that Gal-3, which binds to sugars present on the exterior portion of the PM or the internal portion of intracellular vesicles, has been used as a tool to distinguish ruptured vesicles [44,45].

CHAPTER THREE

MATERIALS AND METHODS

Cell Culture.

The HEK293T and the THP-1 immortalized cell-lines were purchased from the American Type Culture Collection (ATCC). HEK293T and THP-1 cells were cultured at 37°C and 5% CO2 in Dulbecco's modified Eagle's Medium (DMEM) containing phenol red (Invitrogen) or Roswell Park Memorial Institute (RPMI) 1640, supplemented with the 10% fetal bovine serum (FBS) (Hyclone), 10ug/ml ciprofloxacin hydrochloride, 100IU/ml penicillin, and 100ug/ml streptomycin. To generate EV depleted media, FBS was diluted 4x in DMEM or RPMI and was ultracentrifuged for 18 hours, depending on the intended cell type. Afterwards the supernatant was collected and added to either DMEM or RPMI and supplemented with antibiotics.

Differentiation.

THP-1 cells were differentiated into monocyte-derived macrophages by the addition of X phorbol myristate acetate (PMA) (Sigma) at a 1:10000 dilution for 24-48 hours, followed up by RPMI media change sans PMA for 24-48 hours.

Stable Expression of S15 mCherry Construct.

HEK293Tand THP-1 cells were transduced to stably express S15-mCherry using the lentiviral vector (pLVX) backbone containing a CMV promoter to drive the expression of S15-mCherry. Lentiviral particles were generated by polyethylenimine (PEI) transfection of HEK293T cells. The transfection was performed overnight with equal DNA concentrations of VSV-g, ΔNRF or

psPax2, and pLVX-CMV-S15-mCherry plasmid. The next morning the cell medium was changed. The cultured medium from the transfected HEK293T cells was collected 48 hours later and filtered through a 0.45µm syringe filter (Millipore). The purified medium was directly added to THP-1 cells. 72 hours later the cells were selected for expression of our S15-mCherry construct by supplementing DMEM or RPMI 1640 with 5ug/ml puromycin (Hyclone).

Generation of GFP Fusion Protein Constructs.

Expression plasmids containing HIV-1 proteins TAT, VPR, and NEF were all generated by PCR based cloning and restriction enzyme strategies. Primers against TAT, VPR, and NEF proteins were created and either first inserted into the pEGFP-N1 plasmid to create N-terminal GFP fusion constructs of TAT and NEF followed by subcloning into the lentiviral (pLVX) plasmid or directly inserted in pLVX C1-GFP in the case of VPR.

Transfection of HIV-1 GFP Constructs.

HEK293T cells were transfected at approximately 60 percent confluency using Polyethylenimine (PEI), and either pLVX TAT-GFP, GFP-VPR, or NEF-GFP plasmids overnight. The media was changed after overnight transfection and collected 48 hours later. EVs in the cultured media was concentrated via ultracentrifugation as described below.

Immunofluorescence Staining.

In order to adhere EVs to coverslips, either 80µl of resuspended concentrated EV was added to 420µl of PBS totaling 500µl or, for unconcentrated EVs, 500µl of supernatant cultured media was added into the well of 24-well plate containing a glass coverslip (Fischerbrand microscope cover slides, 12-545-J, 22X60-1). Coverslips were initially held in a 50ml conical in 70% ethanol and were added to individual wells of a tissue culture, 24-well plate and subsequently washed with PBS three times. The final round of PBS was left in the well and aspirated immediately

before continuing. The contents of the 24-well plate were spinoculated by centrifugation at 13°C for 2 hours at 1200g onto the coverslips and subsequently fixed in a solution of 0.1 M PIPES containing 3.7% formaldehyde (Polysciences) for 10 minutes and washed 3 times with PBS. The coverslips were permeabilized with a 0.1% solution of saponin in block solution composed of 500mL of PBS supplemented with 10% normal donkey serum (NDS), and 0.01% NaN3 for 5 minutes. After washing 3 times, the coverslips were incubated with rabbit anti-LAMP1 antibodies (Abcam #24170) or rabbit anti-TSG101 (Abcam ab125011) and either mouse anti-CD9 (BD Pharmingen #555370), mouse anti-CD63 (BD Pharmingen #5556019), or mouse anti-CD81 (BD Pharmingen #555675), in the previously stated block solution for 1 hour at room temperature. All primary antibodies were used at 1:1000. In experiments using lectins, biotin conjugated lectins (Vector Laboratories) were used at a working concentration of 5mg/mL in place of primary antibodies for 1.5 hours at room temperature. Afterwards the coverslips were washed with PBS and subsequently incubated with secondary antibodies of conjugated donkey anti-mouse 488 (Jackson ImmunoResearch Laboratories, Inc.) and donkey anti-rabbit 647 (Jackson ImmunoResearch Laboratories, Inc.) at a concentration of 1:400 for 30 minutes at room temperature diluted in PBS block solution and washed with PBS. Additionally, FITC conjugated streptavidin (SAV) (Jackson ImmunoResearch Laboratories, Inc. 016-600-084) at 1:1000 was added for 1 hour at room temperature, diluted in PBS block, and washed with PBS. Afterwards, coverslips were fixed and mounted (Electron Microscopy Sciences, Fluoro-gel with Tris buffer, #17985-11) onto slides (Globe Scientific Inc., Diamond White Glass 25x75x1mm, .5 gloss, #1380-30). In experiments using poly-L-lysine coated coverslips, coverslips were coated by adding 500µl of 0.1% of poly-L-Lysine solution (Sigma Aldrich) to the well and incubated at 37oC for 1 hour. Following incubation, the coverslips were washed 3x with PBS before

continuing with spinoculations.

PKH Dye Labeling of EVs.

EVs from saliva and plasma were isolated as previously described in the collection, preparation and processing methodology section. Similarly, wildtype or S15Ch 293Ts pelleted EVs were concentrated via previously described purification of extracellular vesicle methodology using starting volumes that filled SW28, Beckman Coulter polycarbonate centrifuge tubes (#344058). Afterwards, 293T concentrated EVs were directly resuspended in 100µl of PBS, while saliva and plasma EVs were resuspended in 500µl of PBS overnight on the orbital shake 4oC as described previously. To prepare the EVs for staining, 50µl of either concentrated WT or S15Ch 293T EVs were added to 950µl of Diluent C (Phanos Technologies) while 200µl of concentrated saliva EVs or 500µl of plasma EVs were added to 800µl or 500µl of Diluent C, respectively. Next, a master mix of 0.2µl or 0.4µl of PKH26 or PKH67 (Phanos Technologies) was added to 1ml of Diluent C (Phanos Technologies) per sample to create a final concentration of 200nM or 400nM, respectively. A 200nM PKH67 dye master mix was used for both saliva and plasma EVs. 1ml of the PKH dye master mix was added to the 1ml EVs and Diluent C mixture and was gently pipetted for 30 seconds, followed by being shaken at room temperate on an orbital shaker at 100rpm, for 5 minutes. Afterwards, the reaction was quenched by adding 2ml of 10% BSA (Sigma-Aldrich, #05470) resuspended in PBS. 4.5ml of serum free DMEM was added to the quenched reaction to a total volume of 8.5ml. Next, to minimize turbulence, the 8.5ml mixture was very gently floated on-top of a 1.5ml .971M sucrose (Sigma-Aldrich, #S9378) cushion in a Beckman Coulter polycarbonate centrifuge tube (#349622) and topped off with serum free DMEM. This was followed by centrifugation at 190,000g for 2 hours at 4oC via the SW41 TI rotor to pellet the EVs while removing excess dye. The supernatant and the sucrose cushion were

carefully aspirated, and the pellet was resuspended in 500µl of PBS by gentle pipetting. The resuspended S15Ch or WT 293T pellet was used immediately or stored at -20oC for later use. The resuspended saliva and plasma EVs were stored at -20oC until need and thawed at room temperature. In preparation for imaging, 250µl of the WT or S15Ch resuspension was added to 250µl of PBS and spinoculated onto uncoated coverslips per condition. Conversely, 50µl of the thawed plasma or saliva EVs were added to 450µl of PBS and spinoculated onto 0.1% Poly-L-Lysine (Sigma Aldrich) coated coverslips as described previously. EVs were then subjected to immunofluorescence staining as described in immunofluorescence staining methodology section.

In Vitro NLRP3 Inflammasome Activation.

Differentiated THP-1 cells were plated in 6 well, 60mm, or 10cm plates and stimulated with the indicated stimuli. Cells were primed with 10 ng/mL LPS (from E. coli 055:B5, Sigma-Aldrich) for 4h followed by 5 mM ATP (Invivogen) for 3h.

CHAPTER FOUR

RESULTS

As shown in our recently published paper, we have developed a technique to allow for evaluation of heterogenous EV populations on an individual level (46). This image-based workflow aided by fluorescent microscopy is used to characterize EVs via Multiplexed Analysis of Co-localization, or EV-MAC. With this technique, we are able to characterize EVs from different cell types, as well as analyze differences in the distribution of various EV markers in said populations. It is with this technique that we are able to more definitively analyze EV populations under different inflammatory inductions, which will be described later on.

Initially, we had to demonstrate the effectiveness of EV-MAC in being able to elucidate differences in EV populations containing different cargos. To do this, we used GFP-tagged versions of various HIV-1 proteins, such as Tat, Vpr, and Nef. These proteins have been shown as cargo associated with EVs released from HIV-1 infected cells [47]. These constructs were transfected into 293Ts, and media from the cells was collected after the allotted time. EVs were spun onto coverslips, stained, and then visualized microscopically. Surfaces around the GFP-tagged proteins were built as described previously, and to each surface we analyzed colocalization with various EV markers such as CD9, CD63, CD81, and LAMP1, as well as TSG101 which has been stated to be incorporated into EV membranes. The localization patterns were quantified and graphed in Figure 5. As evident, different HIV-1 proteins released were associated with different distributions of EV markers. These data support the sensitivity of our

technique and our ability to specifically quantify cargos associated with EVs released from cells, as confirmed by colocalization with various EV markers.

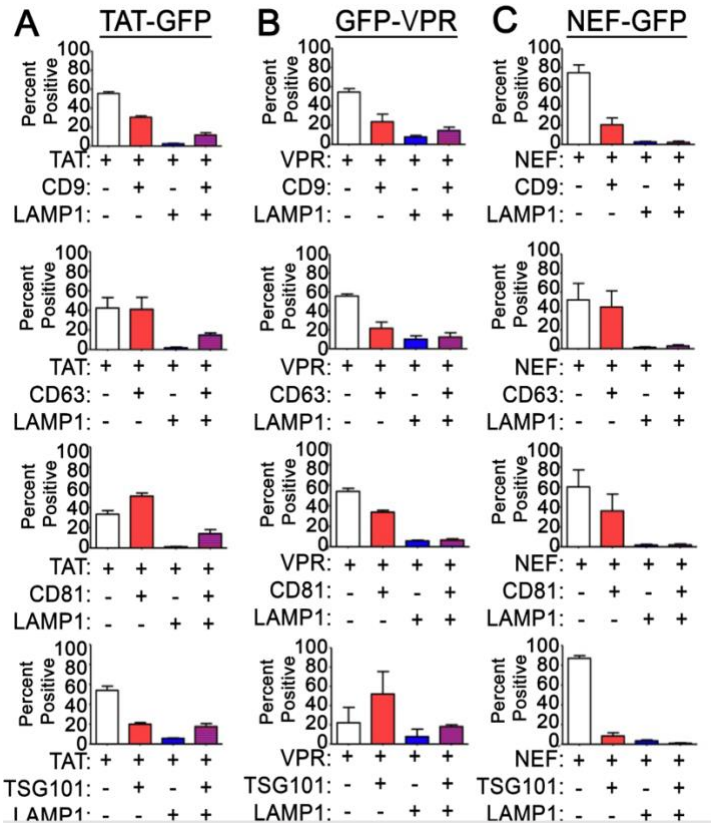

Figure 5. EVs Associated with Different HIV-1 Proteins Have Different Distributions of Pan-EV Markers (46). The degree of co-localization of (A) TAT-GFP, (B) GFP-VPR, and (C) NEF-GFP EVs with tetraspanin markers, LAMP1 and TSG101. The data shown is the mean value from three independent media preparations and coverslips in which pooled data from a single coverslip was used to determine the mean co-localization percentages. Error bars show the standard error of the mean.

Lectins bind to carbohydrates of different sugar linkages that are present on both glycoproteins and glycolipids that make up EVs. Our interest progressed further to see if we can use lectins to stain for these linkages, and thus be useful as additional EV markers. To confirm which lectins would be the best EV marker, we examined the glycan composition associated with our S15Ch+ EVs by staining with various biotinylated lectins under two conditions: normal, and under conditions where lysosome acidification has been disrupted, such that EVs released

from cells have altered composition[48]. Figure 6 shows the diversity in lectin distribution amongst our S15Ch+ EVs, and how lectin composition is affected under various stimuli. This supports the notion that some lectins could be used as comprehensive EV markers, and their distribution would change accordingly with differing stimuli.

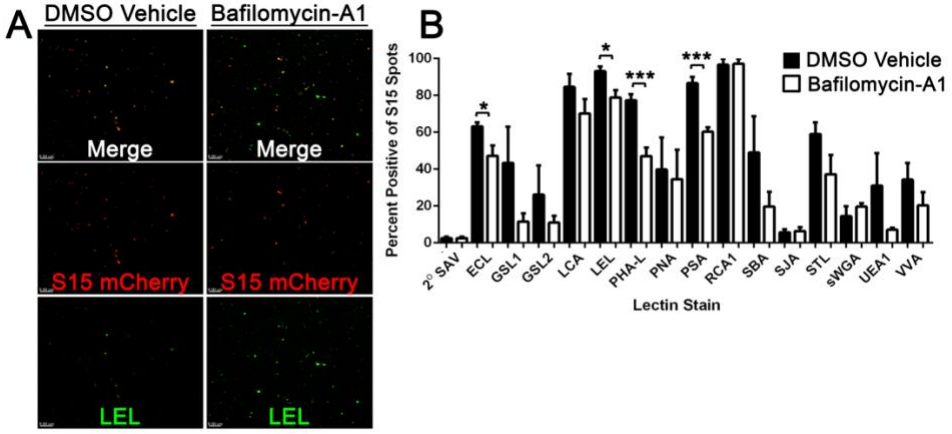

Figure 6. S15Ch+ EVs and Lectins Colocalize Under Normal and Lysosome-Inhibited States (46). A) The cultured media from S15Ch 293Ts was incubated with the indicated biotinylated lectins followed by Alexa 488 streptavidin to determine the glycan profile of EVs under both DMSO Vehicle (DMSO) and 100nM Bafilomycin-A1 (BafA1) treated conditions. B) Data shown is the mean percent co-localization summation of at least three independent media preparations and coverslips. Significant differences between control and BafA1 treated samples were determined via two-tailed T-test. * = p-value < .05, ** = p-value < .01, *** = p-value < .001.Error bars show standard error of the mean.

So far, we have used pan EV markers such as tetraspanins to stain for EVs released from cells, and have shown that some lectins bind highly to carbohydrate structures present on EVs of certain cell types, with lectin distributions varying under different conditions. Our next aim was to confirm the effectiveness of fluorescent membrane dyes in labeling EV populations. PKH dyes are fluorescent lipophilic dyes, in which the aliphatic tail of the dye binds to exposed lipid bilayers. This interaction is maintained by long term, strong noncovalent interactions [49]. Via lateral diffusion, entire cell membranes can be stained with this dye, thus making them very useful in cell labeling. We collected EVs from 293Ts, concentrated them, and incubated them

with PKH26 membrane dye using concentrations of 200nM and 400nM. Excess dye was removed, and we proceeded to spinoculate EVs onto coverslips as previously mentioned, while staining for CD81 and LAMP1. We also used the dye with our S15Ch+ EVs, and saw that while 50% of the PKH puncta were S15Ch+ positive, all the S15Ch+ EVs were positive for the dye. This suggests that the dye is potentially staining additional EVs that our S15Ch+ construct isn't incorporated in, or at least to the strength that would be detected by our microscope. Results from this experiment are shown in Figure 7 below. Worth noting is that non-EV associated fluorescent structures have been noted to form, some much larger in size and some similar in size to EVs. The dye forms micelles when not in the presence of structures to take up the dye. Hence, there needs to be an appropriate dye-to-protein ratio when proceeding with PKH dye staining. Additionally, it's been shown that a sucrose gradient following ultracentrifugation eliminates these larger micelle structures. Unfortunately, it's harder to differentiate between the non-EV structures that are similar in size to the EVs that have taken up the dye. The PKH dye should be used with a determined protein concentration, and canonical EV markers can further aid in confirming whether PKH positive puncta are true EVs or not.

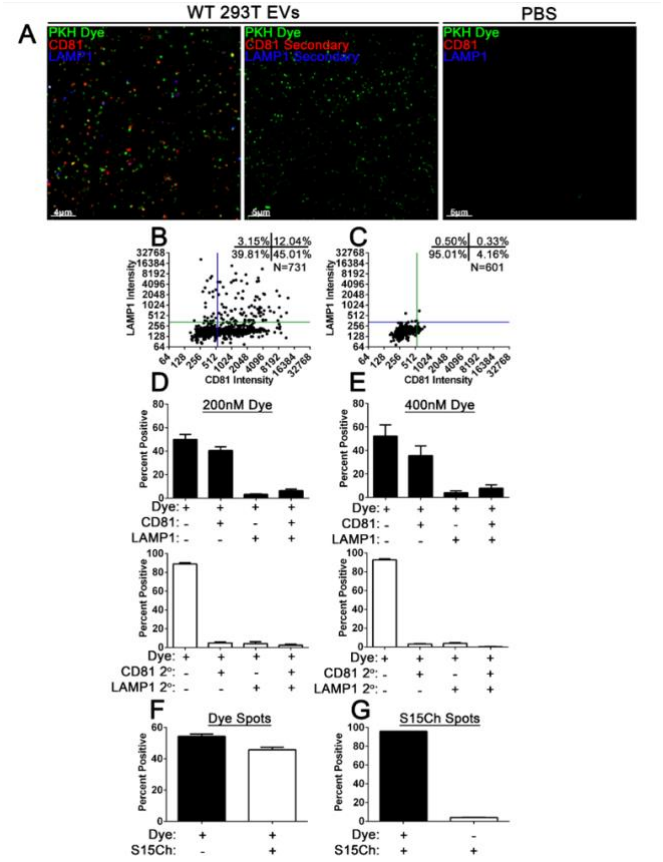

Figure 7. PKH Stained EVs from 293Ts Colocalize with CD81 and LAMP1, and Identify S15Ch+ EVs (46). Concentrated EVs from WT 293T cells or PBS were dyed with PKH26 (PKH Dye, green) at an initial dye concentration of 200nM or 400nM. A) Representative z-stack from WT 293T EVs or PBS demonstrating co-localization of PKH Dye(green), CD81(red), and LAMP1(Blue) or its respective secondary antibody control. The dye labelled EVs were imaged and 3D reconstructions were used to identify dye positive EVs using the same spots masking algorithm for both dye concentrations to determine their co-localization with CD81 and LAMP1. B, C) Representative co-localization from a 200nM PKH dye image demonstrate relative co-localization. A total of three (D) and five (E) independent replicates were conducted for the 200nM and 400nM conditions, respectively. 10-15 images were taken per coverslip for each condition for each replicate. The number of EVs identified per image ranged from ~200-780. Concentrated S15Ch 293T EVs were either dyed with PKH67 (Dye) with an initial dye concentration of 200nM or remained unstained. Both the undyed and dye labelled S15Ch EVs were then imaged, and 3D reconstructions were used to generate a spots masking algorithm around the dye positive (F) or S15Ch positive (G) EVs. F) The percent of Dye+ EVs, as identified by its spots, demonstrate that the S15Ch could be reproducible found within the concentrated EVs. G) The percent of S15Ch positive EVs, as identified by its spots algorithm, show their co-localization with the dyed EVs (left) are undyed EVs (right). three independent replicates were conducted. 10-15 images were taken per replicate. The number of identified Dye EVs per image ranged, from ~1100-1500; number of S15Ch identified EVs per image ranged, ~350-600. All data shows the mean value among replicates, error bars show the standard error of the mean.

Before progressing to the analysis of EVs released under inflammatory conditions, we wanted to also verify the accuracy of our microscopy techniques, specifically the binning settings we chose for our images. Modern digital cameras have a charged coupled device photon detector, which captures and stores image information in the form of localized electrical charge. Each electrical charge signal corresponds with a different light intensity. Each one of these signals is associated with a picture element, or a pixel, and each signal is read out quickly as an intensity value for that specific location. These values become quickly digitized and form the image we see on screen. Additionally, each pixel can be thought of as a well of electrons, and when that well becomes filled, pixels lose their ability to accommodate any additional charge. That charge can then be spread to neighboring pixels, which can give the impression of incorrect values or allow neighboring pixels themselves to reach saturation. With all that in mind, binning is the concept of combining charge from adjacent pixels. Binning ensure that Signal-to-noise ratio is lower, and at higher binning photos are digitized faster. We wanted to confirm that our binning setting of 2x2 doesn't affect our picture resolution versus a binning of 1x1. The overall trends we saw for our S15Ch+ puncta weren't affected in a binning of 2x2 vs. a binning of 1x1, as seen in Figure 8.

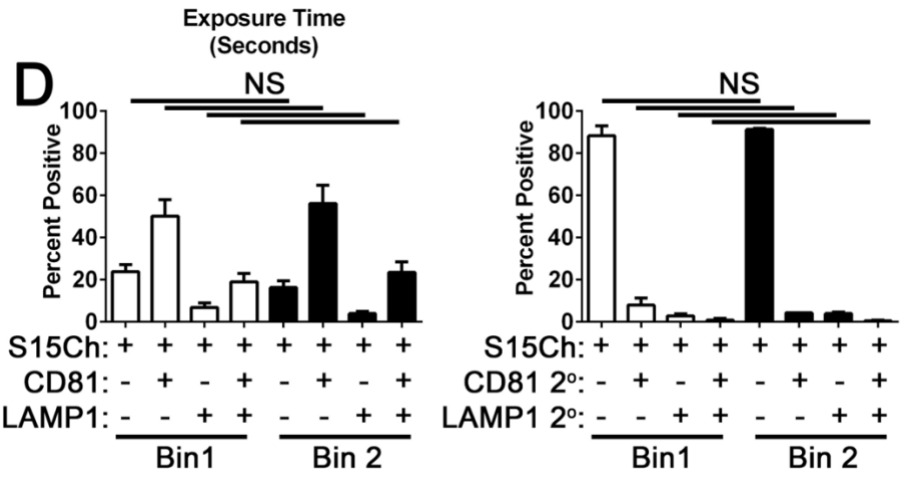

Figure 8. S15Ch+ Puncta Colocalized with CD81 and LAMP1 from Bin 1x1 and Bin 2x2 Collected Fields (46). D) S15Ch co-localization distribution for S15Ch EVs stained with CD81 and LAMP1 from Bin 1x1 and Bin 2x2 collected fields. 12 images were taken per coverslip. All data shows the mean value among replicates, error bars show the standard error of the mean.

With an established system in visualizing, quantifying, and analyzing EVs, we then turned our sights into applying these methods to analyze EV populations under both normal and inflammatory conditions. As mentioned earlier while discussing inflammation, NLRP3 inflammasome activation, driven by caspase-1, leads to a plethora of proteins being released from cells, more so than when the inflammasome isn't activated. We wished to analyze these EV populations under normal conditions vs. conditions where the NLRP3 inflammasome was active. Accepted modes of NLRP3 activation include priming cells with LPS for 4 hours, and then following up with agonists such as ATP, anywhere from 30 minutes to 3 hours.

To confirm the inflammasome was truly activated upon our LPS/ATP treatments, supernatant from differentiated THP-1 cells after 4 hours LPS/ 1 hour ATP treatments was collected. Throughout the treatments, cells were observed microscopically to ensure cells weren't pyroptotic, and LDH assays done by other lab members have showed that these treatment times don't induce pyroptosis (Data not shown). Upon collection, supernatant was spun down at 3000 x g for 10 minutes to eliminate any potential cell debris. Afterwards, that

supernatant was collected and saved. An ELISA was run on that supernatant, looking for IL-1β levels that were quantifiably larger under LPS/ATP treatment vs. no treatment. IL-1β secretion from the ELISA are shown in figure 9 below.

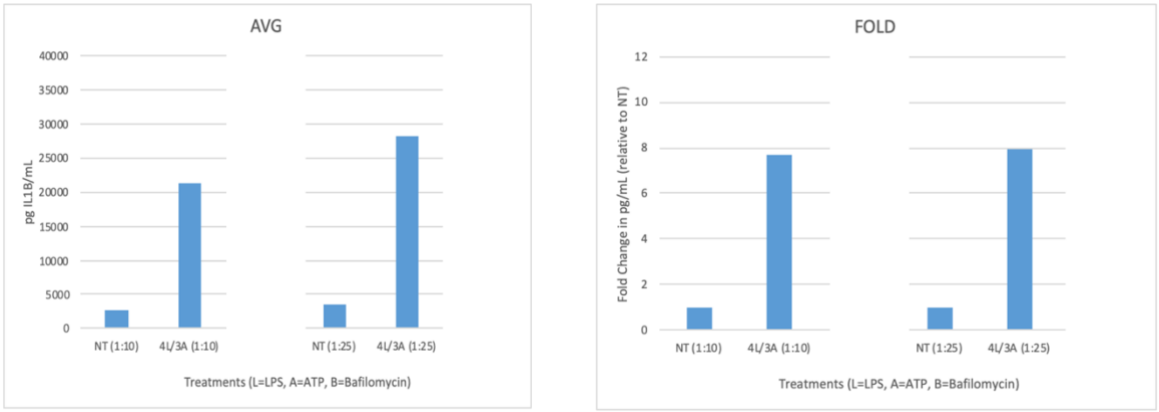

Figure 9. NLRP3 Inflammasome Activation Asserts Noticeable Increase in IL-1β Release. Differentiated THP-1's were either not treated, or treated with LPS for 4 hours followed by ATP for 3 hours. Supernatant was collected from cells, and an IL-1ß ELISA was run on the supernatant with two dilutions: 1:10 and 1:25.

With the confirmation that we indeed activate the inflammasome with our treatments, we now can analyze EV released from these cells by staining them for various markers of our choosing. Figure 10 below demonstrates an example of the type of analyzations we can conduct with our approach. We see a substantially greater number of puncta under the 4 hours LPS/ 3 hours ATP treatment versus when we don't treat the cells with priming and activating signals. Additionally, one can appreciate that the distribution of markers is also altered under inflammasome activation versus when the inflammasome is not active. It is these differences that can be beneficial upon distinguishing EVs from normal versus pathological conditions. These analyses can be done with a large variety of markers to gate on and other cargoes to stain for, and future potential experiments are further described in Chapter Five.

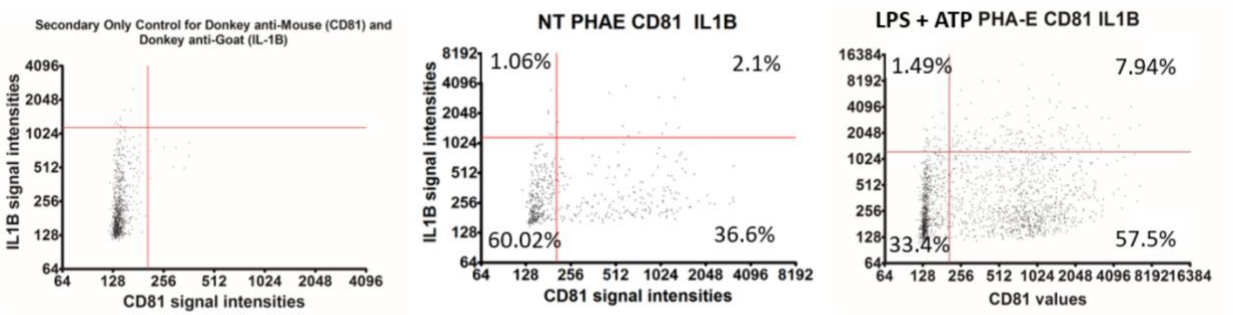

Figure 10. Tetraspanin CD81 and Cytokine IL-1β Gated Around Lectin PHAE Under Both No Treatment Conditions vs. Inflammasome Activation. An average of 10-15 images were taken for each condition. Left most graph indicates secondary only antibody control, middle indicates no treatment (NT) and right most graph under LPS+ ATP treatment. Percent triple positive, i.e. puncta gated around PHAE that were also positive for IL-1β and CD81, were roughly 4 times larger under the inflammasome activating treatments compared to NT. A larger percentage of released EVs were also positive for PHAE and CD81 under inflammasome activation compared to NT.

CHAPTER FIVE

DISCUSSION AND FUTURE DIRECTIONS

Using quantitative fluorescent microscopy, we are able to navigate through different EV populations, applying accepted notions in the field towards more novel and elusive approaches. Our approach is straight-forward and allows for the heterogeneity of EV populations to more clearly be defined, versus other approaches that either don't encompass the heterogeneity, or require far more advanced technology that is not always easily accessible. By building surfaces around our proposed EVs and then confirming them by staining for various markers, we are able to analyze thousands of EVs rather quickly. Additionally, we can analyze them in a cargo-specific manner, and differences between populations carrying different cargos can be beneficial in examining pathogenic EVs. Using other approaches to label EVs, such as with lectins and PKH membrane dyes, further emphasizes the versatility EV-MAC can incorporate.

There are many exciting avenues to continue exploring with our EV-MAC categorizing techniques. Of course, established EV markers such as tetraspanins and ESCRT proteins have long been used in the field. We are very excited about the utilization of lectins for further analyzation of carbohydrate enriched areas on EVs. A caveat to the approach using lectins, and one that we fortunately caught early on, is that lectins recognize glycosylated regions on carbohydrates, and antibodies we use to label certain markers or cargos are also glycosylated. Hence, we ran into the problem that the lectins may have been recognizing antibody structures, and thus some of our colocalization may not have been entirely accurate. To circumvent this problem, we have ordered antibodies lacking the Fc portion of the antibody structure, which is

the most glycosylated part of the antibody, in hopes that this issue would be somewhat more controlled. Additionally, we will be optimizing our staining techniques, such that lectin staining would take place prior to antibody staining. Lastly, we can use fluorescently conjugated proteins that don't require antibody staining to use for our lectin staining experiments. There is a lot of potential with the lectin staining, and we are very excited about the prospect of categorizing a diverse range of EVs from different cell types and environments and seeing how their carbohydrate composition is altered. This can further give us insight as to the role these EVs have in regard to cell-to-cell communication and fusion with target cells.

The membrane dye also carries potential for future experiments. We have shown that the dye labels all of our S15Ch+ puncta, which we expect to be incorporated into various membranes. Interestingly, only 50% of the dye puncta are positive for the S15Ch+ puncta. This raises a few interesting questions. The quality of our S15Ch transfections will always vary, and it's difficult to conceive a widespread 100% effective transfection. It is possible that there was some S15Ch signal present with dye puncta, however maybe not strong enough for our scope to detect it, or more simply that our S15Ch as mentioned just wasn't incorporated into all membranes. We expect that most of the 50% of the dye that wasn't positive for S15Ch+ are EVs, with some dye-forming micelles which to the best of our abilities we simply aren't able to exclude. While it doesn't give us the carbohydrate-defining distributions our lectin staining provides, it does stain proposed EVs well, and allows us to stain for other cargos or markers concurrently without having to worry about the problems we ran into with the lectins.

As mentioned, of specific interest to me is utilizing EV-MAC for studying inflammation. A multitude of proteins are released from cells upon inflammatory induction, and many bypass the conventional protein secretion pathway, thus taking other routes to be released from host

cells. Using our EV labeling approaches, we can stain for various markers as long as we have the available antibodies to them. We can stain for different inflammasome-related components and see if more are released under inflammatory induction, and how the distribution of markers is altered upon such inductions as well. I've demonstrated the type of experiments we would conduct in Figure 10. As stated, we wouldn't be able to repeat this experiment again while using a lectin and staining for cargos using antibodies without further protocol optimization. However, it stands to reason based on the trend we saw and what's been shown in the literature that EV compositions should be altered upon inflammatory induction, even when just considering the proteins released under inflammasome activated conditions versus normal.

There were many additional experiments that, due to unforeseen circumstances, couldn't be completed. Referring back to using EV-MAC to study EVs released under normal versus inflammasome activated conditions, I would be curious to stain for other proteins that have been shown to be released extracellularly and see if they are associated with EVs. Such proteins would be NLRP3, Caspase-1, and ASC. ASC in particular holds the most interest to us.

As described in Chapter Two, ASC forms these defined, speck like puncta within cells under inflammasome activation, and these specks have also been found extracellularly. There are many questions we would like to ask regarding the functions of this extracellular ASC, as it has been shown to exhibit prion-like qualities. We would answer these questions using an ASC-GFP THP-1 cell line, where ASC would be fluorescently tagged with GFP. By treating with our NLRP3 inflammasome activators LPS + ATP, we would be able to visualize green ASC puncta within the cell, versus a diffuse green in cells that weren't treated with LPS + ATP. Our first question would be if extracellular ASC is released from cells in the context of EVs. We would use EV-MAC to answer this. We would collect supernatant from ASC-GFP treated cells, spin

them down onto coverslips, and stain for various EV markers, stain for lectins, or use our membrane dye. We can gate around our GFP+ puncta, and see colocalization patterns with our other markers, or we can gate around our EV markers and see how much ASC colocalizes with them. With either method, we would be able to definitely show that ASC is or isn't released in the context of EVs. Regardless of whether it is or isn't released with EVs, we can still explore the prion like qualities of ASC. We can add concentrated supernatant of ASC-GFP to cells that express ASC-mCherry. One would expect that exogenous ASC-GFP wouldn't be able to degrade upon entering the host cell, which begs the question: What does it do upon endocytosis? Would we see ASC-GFP interacting with endogenous ASC-mCherry? What happens to exogenous ASC upon uptake? Our lab has shown that when α-synuclein is taken up by target cells and sorted within endosomes, we see vesicular rupture as evident by gal-3 colocalization. It would be fascinating if we saw something similar with ASC taken up and using an endogenously expressed gal-3-mCherry to confirm vesicular rupture. Our approach for analyzing EVs can assist in answering and elucidating many previously discussed observations, and I look forward to seeing where these experiments unfold with future students.

REFERENCE LIST

1. Netea MG, Schlitzer A, Placek K, Joosten LAB, Schultze JL. Innate and Adaptive Immune Memory: an Evolutionary Continuum in the Host's Response to Pathogens. *Cell Host and Microbe*. 2019;25(1):13-26. doi:10.1016/j.chom.2018.12.006

2. Eren E, Özören N. The NLRP3 inflammasome: A new player in neurological diseases. *Turkish Journal of Biology*. 2019;43(6):349-359. doi:10.3906/biy-1909-31

3. Yim WWY, Mizushima N. Lysosome biology in autophagy. *Cell Discovery*. 2020;6(1). doi:10.1038/s41421-020-0141-7

4. Kielian T. Lysosomal storage disorders: pathology within the lysosome and beyond. *Journal of Neurochemistry*. 2019;148(5):568-572. doi:10.1111/jnc.14672

5. Cypryk W, Nyman TA, Matikainen S. From inflammasome to exosome - Does extracellular vesicle secretion constitute an inflammasome-dependent immune response? *Frontiers in Immunology*. 2018;9(SEP). doi:10.3389/fimmu.2018.02188

6. Quek C, Hill AF. The role of extracellular vesicles in neurodegenerative diseases. *Biochemical and Biophysical Research Communications*. 2017;483(4):1178-1186. doi:10.1016/j.bbrc.2016.09.090

7. Kelley N, Jeltema D, Duan Y, He Y. The NLRP3 inflammasome: An overview of mechanisms of activation and regulation. *International Journal of Molecular Sciences*. 2019;20(13). doi:10.3390/ijms20133328

8. Martinon F, Burns K, Tschopp J. The Inflammasome: A molecular platform triggering activation of inflammatory caspases and processing of proIL-β. *Molecular Cell*. 2002;10(2). doi:10.1016/S1097-2765(02)00599-3

9. Keller M, Rüegg A, Werner S, Beer HD. Active Caspase-1 Is a Regulator of Unconventional Protein Secretion. *Cell*. 2008;132(5). doi:10.1016/j.cell.2007.12.040

10. Eder C. Mechanisms of interleukin-1β release. *Immunobiology*. 2009;214(7). doi:10.1016/j.imbio.2008.11.007

11. Kim J, Gee HY, Lee MG. Unconventional protein secretion – new insights into the pathogenesis and therapeutic targets of human diseases. *Journal of Cell Science*. 2018;131(12). doi:10.1242/jcs.213686

12. Dinarello CA. Overview of the IL-1 family in innate inflammation and acquired immunity. *Immunological Reviews*. 2018;281(1). doi:10.1111/imr.12621

13. Lopez-Castejon G, Brough D. Understanding the mechanism of IL-1β secretion. *Cytokine and Growth Factor Reviews*. 2011;22(4). doi:10.1016/j.cytogfr.2011.10.001

14. Välimäki E, Cypryk W, Virkanen J, et al. Calpain Activity Is Essential for ATP-Driven Unconventional Vesicle-Mediated Protein Secretion and Inflammasome Activation in Human Macrophages. *The Journal of Immunology*. 2016;197(8). doi:10.4049/jimmunol.1501840

15. Franklin BS, Latz E, Schmidt FI. The intra-and extracellular functions of ASC specks. *Immunological Reviews*. 2018;281(1). doi:10.1111/imr.12611

16. Stancu IC, Cremers N, Vanrusselt H, et al. Aggregated Tau activates NLRP3–ASC inflammasome exacerbating exogenously seeded and non-exogenously seeded Tau pathology in vivo. *Acta Neuropathologica*. 2019;137(4). doi:10.1007/s00401-018-01957-y

17. Burton EM, Goldbach-Mansky R, Bhaduri-McIntosh S. A promiscuous inflammasome sparks replication of a common tumor virus. *Proceedings of the National Academy of Sciences of the United States of America*. 2020;117(3). doi:10.1073/pnas.1919133117

18. Gavrilin MA, McAndrew CC, Prather ER, et al. Inflammasome Adaptor ASC Is Highly Elevated in Lung Over Plasma and Relates to Inflammation and Lung Diffusion in the Absence of Speck Formation. *Frontiers in Immunology*. 2020;11. doi:10.3389/fimmu.2020.00461

19. Linden R. The biological function of the prion protein: A cell surface scaffold of signaling modules. *Frontiers in Molecular Neuroscience*. 2017;10. doi:10.3389/fnmol.2017.00077

20. Wulf MA, Senatore A, Aguzzi A. The biological function of the cellular prion protein: An update. *BMC Biology*. 2017;15(1). doi:10.1186/s12915-017-0375-5

21. Castle AR, Gill AC. Physiological functions of the cellular prion protein. *Frontiers in Molecular Biosciences*. 2017;4(APR). doi:10.3389/fmolb.2017.00019

22. Kupfer L, Hinrichs W, Groschup M. Prion Protein Misfolding. *Current Molecular Medicine*. 2009;9(7). doi:10.2174/156652409789105543

23. Glick D, Barth S, Macleod KF. Autophagy: Cellular and molecular mechanisms. *Journal of Pathology*. 2010;221(1). doi:10.1002/path.2697

24. Marques ARA, Saftig P. Lysosomal storage disorders – challenges, concepts and avenues for therapy: Beyond rare diseases. *Journal of Cell Science*. 2019;132(2). doi:10.1242/jcs.221739

25. Zheng J, Tan J, Miao YY, Zhang Q. Extracellular vesicles degradation pathway based autophagy lysosome pathway. *American Journal of Translational Research*. 2019;11(3).

26. Maas SLN, Breakefield XO, Weaver AM. Extracellular Vesicles: Unique Intercellular Delivery Vehicles. *Trends in Cell Biology*. 2017;27(3):172-188. doi:10.1016/j.tcb.2016.11.003

27. Cocucci E, Racchetti G, Meldolesi J. Shedding microvesicles: artefacts no more. *Trends in Cell Biology*. 2009;19(2). doi:10.1016/j.tcb.2008.11.003

28. Caruso S, Poon IKH. Apoptotic cell-derived extracellular vesicles: More than just debris. *Frontiers in Immunology*. 2018;9(JUN). doi:10.3389/fimmu.2018.01486

29. Doyle L, Wang M. Overview of Extracellular Vesicles, Their Origin, Composition, Purpose, and Methods for Exosome Isolation and Analysis. *Cells*. 2019;8(7). doi:10.3390/cells8070727

30. Poon IKH, Lucas CD, Rossi AG, Ravichandran KS. Apoptotic cell clearance: Basic biology and therapeutic potential. *Nature Reviews Immunology*. 2014;14(3). doi:10.1038/nri3607

31. Muhsin-Sharafaldine MR, Saunderson SC, Dunn AC, Faed JM, Kleffmann T, McLellan AD. Procoagulant and immunogenic properties of melanoma exosomes, microvesicles and apoptotic vesicles. *Oncotarget*. 2016;7(35). doi:10.18632/oncotarget.10783

32. Słomka A, Urban SK, Lukacs-Kornek V, Żekanowska E, Kornek M. Large Extracellular Vesicles: Have We Found the Holy Grail of Inflammation? *Frontiers in immunology*. 2018;9. doi:10.3389/fimmu.2018.02723

33. Borges FT, Reis LA, Schor N. Extracellular vesicles: Structure, function, and potential clinical uses in renal diseases. *Brazilian Journal of Medical and Biological Research*. 2013;46(10). doi:10.1590/1414-431X20132964

34. Fader CM, Colombo MI. Autophagy and multivesicular bodies: Two closely related partners. *Cell Death and Differentiation*. 2009;16(1):70-78. doi:10.1038/cdd.2008.168

35. Lozano-Andrés E, Libregts SF, Toribio V, et al. Tetraspanin-decorated extracellular vesicle-mimetics as a novel adaptable reference material. *Journal of Extracellular Vesicles*. 2019;8(1). doi:10.1080/20013078.2019.1573052

36. Kowal J, Arras G, Colombo M, et al. Proteomic comparison defines novel markers to characterize heterogeneous populations of extracellular vesicle subtypes. *Proceedings of the National Academy of Sciences of the United States of America*. 2016;113(8):E968-E977. doi:10.1073/pnas.1521230113

37. Willms E, Cabañas C, Mäger I, Wood MJA, Vader P. Extracellular vesicle heterogeneity: Subpopulations, isolation techniques, and diverse functions in cancer progression. *Frontiers in Immunology*. 2018;9(APR). doi:10.3389/fimmu.2018.00738

38. Andreu, Z., Yanez-Mo, M. Tetraspanins in Extracellular Vesicle Formation and Function. *Frontiers of Immunology.* https://www.frontiersin.org/articles/10.3389/fimmu.2014.00442/full . 2014.

39. Willms E, Johansson HJ, Mäger I, et al. Cells release subpopulations of exosomes with distinct molecular and biological properties. *Scientific Reports*. 2016;6. doi:10.1038/srep22519

40. Bissig C, Gruenberg J. ALIX and the multivesicular endosome: ALIX in Wonderland. *Trends in Cell Biology*. 2014;24(1). doi:10.1016/j.tcb.2013.10.009

41. Klingborne et al. Role of exosomes in normal and diseased eye. *Prog Ret Eye Res*. https://www.semanticscholar.org/paper/Roles-of-exosomes-in-the-normal-and-diseased-eye-Klingeborn-Dismuke/0d2c33640edb6ef05d421eee98a0748f021c8b43 (2017)

42. Williams C, Royo F, Aizpurua-Olaizola O, et al. Glycosylation of extracellular vesicles: current knowledge, tools and clinical perspectives. *Journal of Extracellular Vesicles*. 2018;7(1). doi:10.1080/20013078.2018.1442985

43. Hart GW, Akimoto Y. Essentials of Glycobiology. 2nd edition. *Essentials of Glycobiology 2nd edition*. Published online 2009.

44. Flavin WP, Bousset L, Green ZC, et al. Endocytic vesicle rupture is a conserved mechanism of cellular invasion by amyloid proteins. *Acta Neuropathologica*. 2017;134(4). doi:10.1007/s00401-017-1722-x

45. Freeman D, Cedillos R, Choyke S, et al. Alpha-Synuclein Induces Lysosomal Rupture and Cathepsin Dependent Reactive Oxygen Species Following Endocytosis. *PLoS ONE*. 2013;8(4). doi:10.1371/journal.pone.0062143

46. Burbidge, K., Zwikelmaier, V., Cook, B., Long, M., Balva, B**.,** Longiro, M., Ispas, G., Rademacher, D.J., Campbell, E.M.. Cargo and Cell Specific Differences in Extracellular Vesicle Populations Identified by Multiplexed Immunofluorescent Analysis. *Journal of Extracellular Vesicles.* July 17th, 2020.

47. Madison MN, Okeoma CM. Exosomes: Implications in HIV-1 pathogenesis. *Viruses*. 2015;7(7). doi:10.3390/v7072810

48. Villarroya-Beltri C, Baixauli F, Mittelbrunn M, et al. ISGylation controls exosome secretion by promoting lysosomal degradation of MVB proteins. *Nature Communications*. 2016;7. doi:10.1038/ncomms13588

49. Pužar Dominkuš P, Stenovec M, Sitar S, et al. PKH26 labeling of extracellular vesicles: Characterization and cellular internalization of contaminating PKH26 nanoparticles. *Biochimica et Biophysica Acta - Biomembranes*. 2018;1860(6). doi:10.1016/j.bbamem.2018.03.013

VITA

Barak Balva was born in Tiberias, Israel, on February 22nd, 1992 to Eyal and Sigal Balva. His family moved to the United States when he was 5 years old, and settled down in a suburb of Maryland. He attended the University of Delaware in Newark, DE, where he graduated with a Bachelor of Arts in Biology in 2014. For a few years after graduation, he worked for the medical device company ZOLL in NYC before deciding to further his education.

In 2018, Barak matriculated into the Loyola University Chicago Stritch School of Medicine Infectious Diseases and Immunology program. Later on, he joined the lab of Dr. Edward Campbell, where he studied about extracellular vesicles and their role within inflammation. He hopes to continue on with a career in the pharmaceutical industry.